

Results of the stellarator optimization with respect to the neoclassical $1/\nu$ transport*

Bernhard SEIWALD¹⁾, Sergei V. KASILOV^{1,2)}, Viktor V. NEMOV^{1,2)}, Winfried KERNBICHLER¹⁾, Victor TRIBALDOS³⁾, Thomas SUNN PEDERSEN⁴⁾, Victor N. KALYUZHNYI²⁾

¹⁾Association EURATOM-ÖAW, Institut für Theoretische Physik - Computational Physics, TU Graz, Petersgasse 16, A-8010 Graz, Austria

²⁾Institute of Plasma Physics, National Science Center "Kharkov Institute of Physics and Technology", Akademicheskaya Str. 1, 61108 Kharkov, Ukraine

³⁾Asociación Euratom-CIEMAT, Madrid, Spain

⁴⁾Columbia University, Department of Applied Physics and Applied Mathematics, New York, New York 10027, USA

Powerful tools have been developed in the last years for the design of new stellarator devices. These codes are usually working in magnetic coordinates. Tasks addressed by these codes are minimization of neoclassical transport, maximizing equilibrium and stability properties, etc. However, optimizing existing stellarators is time consuming because costly coordinate transformations are involved. A procedure working in real space coordinates for maximizing the plasma energy content, based on reducing the most unfavorable $1/\nu$ neoclassical transport, has been presented in [1]. This tool, named SORSSA, was developed especially for optimizing existing stellarator devices which are not fully optimized with respect to neoclassical transport. Some results for the stellarators Uragan 2M, U-2M, TJ-II and the Columbia Nonneutral Torus, CNT, are presented.

Keywords: Neoclassical Transport, Optimization, Stellarator

1 Introduction

One of the main disadvantages of non-axisymmetric confinement devices is their unfavorable, $1/\nu$, temperature scaling in the long mean free path collisionality (lmfp) regime, $\propto T^{7/2}$. The ∇B drift associated with their three-dimensional asymmetries leads to rapid losses of trapped particles. Therefore, improving stellarator transport starts, precisely, by optimizing the configurations against this disadvantageous $1/\nu$ lmfp regime [2].

2 Energy confinement

The scheme behind SORSSA analyzes the neoclassical $1/\nu$ transport properties of a magnetic field configuration. The measure of the neoclassical transport is the effective ripple ϵ_{eff} [3]. For good confinement ϵ_{eff} should be small. The effective ripple can be used to compute the total stored energy in the plasma volume, which is the figure of merit. The heat conductivity equation is solved under the premise that the neoclassical transport is the dominant transport mechanism. Assuming that the temperature profile is de-

finied by the heat conductivity equation

$$\frac{1}{r} \frac{d}{dr} r \kappa_{\perp} \frac{dT}{dr} + Q(r) = 0, \quad (1)$$

with the boundary conditions $T(a) = 0$ and $\lim_{r \rightarrow 0} \left(r \frac{dT}{dr} \right) = 0$, where a is the boundary of the plasma. The heat conductivity is proportional to $\epsilon_{\text{eff}}^{3/2} T^{7/2}$ and computation of $\epsilon_{\text{eff}}^{3/2}$ for sets of computed magnetic surfaces is an essential part of the optimization procedure. Integrating Eq. (1) leads to the normalized stored energy [4, 5]

$$\hat{W} = \int_0^a dr r \hat{n}(r) \left(\int_r^a \frac{dr'}{r' \epsilon_{\text{eff}}^{3/2}(r')} \right)^{2/9}, \quad (2)$$

where $\hat{n} = n/n_0$ is the normalized particle density profile and a denotes the plasma radius. The integration variable is the effective radius of the flux surfaces. It is convenient to define the re-normalized stored energy W_n as

$$W_n = \hat{W} / \hat{W}_S, \quad (3)$$

with \hat{W} the normalized stored energy defined in Eq. (2) and \hat{W}_S the normalized stored energy of the standard configuration.

The effective ripple $\epsilon_{\text{eff}}^{3/2}$, which is part of the $1/\nu$ neoclassical transport coefficients and contains the characteristic features of the magnetic field geometry, is given by (see [3])

$$\epsilon_{\text{eff}}^{3/2} = \frac{\pi R^2}{8 \sqrt{2}} \lim_{L_s \rightarrow \infty} \left(\int_0^{L_s} \frac{ds}{B} \right) \left(\int_0^{L_s} \frac{ds}{B} |\nabla \psi| \right)^{-2}$$

*This work, supported by the European Communities under the contract of Association between EURATOM and the Austrian Academy of Sciences, was carried out within the framework of the European Fusion Development Agreement. The views and opinions expressed herein do not necessarily reflect those of the European Commission. Additional funding is provided by the Austrian Science Foundation, FWF, under contract number P16797-N08.

author's e-mail: seiwald@itp.tugraz.at

$$\int_{B_{min}^{(abs)}/B_0}^{B_{max}^{(abs)}/B_0} db' \sum_{j=1}^{j_{max}} \frac{\hat{H}_j^2}{\hat{I}_j} \quad (4)$$

with

$$\hat{H}_j = \frac{1}{b'} \int_{s_j^{(min)}}^{s_j^{(max)}} \frac{ds}{B} \sqrt{b' - \frac{B}{B_0}} \left(4 \frac{B_0}{B} - \frac{1}{b'} \right) |\nabla\psi| k_G \quad (5)$$

$$\hat{I}_j = \int_{s_j^{(min)}}^{s_j^{(max)}} \frac{ds}{B} \sqrt{1 - \frac{B}{B_0 b'}} \quad (6)$$

and $b' = v^2/J_{\perp} B_0$. The geodesic curvature of the magnetic field line is given as $k_G = (\mathbf{h} \times (\mathbf{h} \cdot \nabla)\mathbf{h}) \cdot \nabla\psi/|\nabla\psi|$ with the unit vector $\mathbf{h} = \mathbf{B}/B$. Equation (4) is computed by integration over the magnetic field line, s , over a sufficiently large interval $0 - L_s$, and by integration over the perpendicular adiabatic invariant of trapped particles, J_{\perp} . Here, $B_{min}^{(abs)}$ and $B_{max}^{(abs)}$ are the minimum and maximum values of B within the interval $[0, L_s]$. The quantities $s_j^{(min)}$ and $s_j^{(max)}$ within the sum over j in (4) - (6) correspond to the turning points of trapped particles. This integration takes into account all kinds of trapped particles, such as those trapped within one magnetic field ripple as well as particles trapped within several magnetic field ripples.

The total stored energy, defined in Eq. (2), depends on ϵ_{eff} and on the plasma volume. A decrease of ϵ_{eff} at a fixed plasma volume increases the stored energy as well as an increase of the plasma volume at a fixed value of ϵ_{eff} . As the plasma volume and ϵ_{eff} are not independent in a stellarator, the optimum stored energy will not necessarily coincide with the largest attainable volume or at the lowest possible value of ϵ_{eff} .

3 Application

The total stored energy, defined in Eq. (2), has been used as figure of merit for optimizing the stellarators U-2M, TJ-II and CNT.

The U-2M device [6] is an $l = 2$ torsatron. An additional toroidal magnetic field is produced by a system of 16 toroidal field coils (TF coils) which are uniformly distributed in angle along the major circumference (four coils in each field period). The mean current in such a coil, I_{TFC} , is expressed in units of the helical winding current. For the standard configuration this current is $I_{TFC} = 5/12$, according Ref. [6]. In this case the parameter $k_{\varphi} = B_{th}/(B_{th} + B_{tr})$ is $k_{\varphi} = 0.375$ where B_{th} and B_{tr} are the toroidal components of the magnetic field produced by the helical winding and TF coils, respectively.

The vertical field coil (VF coil) system plays an important role in achieving the magnetic configuration of the torsatron. The total vertical magnetic field, B_{\perp} , is produced by the VF coils and the vertical magnetic field of the helical

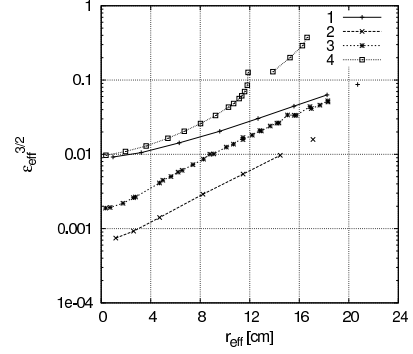


Fig. 1 Parameters $\epsilon_{eff}^{3/2}$ as functions of r_{eff} for $k_{\varphi} = 0.31$ and various f_{VFC} ; 1: $f_{VFC} = 1$, $\Delta I = 0$; 2: $f_{VFC} = 1.166$ ($B_{\perp}/B_0 = 0$), $\Delta I = 0$; 3: $f_{VFC} = 1$, $\Delta I = 0.06$; 4 (standard configuration): $k_{\varphi} = 0.375$, $f_{VFC} = 1$, $\Delta I = 0$. (taken from [1])

winding. The desired vertical field is obtained by adjusting the current in the VF coils. In the computations the VF coil system variant [7] is used which allows to suppress significantly the island structure of the magnetic surfaces.

Three control parameters are appropriate for the optimization. These parameters are related to the currents in the helical winding and in TF as well as VF coils:

(i) I_{TFC} , the mean current of TF coils, in units of helical winding current. It is directly connected to the above mentioned parameter k_{φ} (used in Refs. [6, 8]) by the ratio $k_{\varphi} = 1/(1 + 4I_{TFC})$ as it follows from the k_{φ} definition.

(ii) ΔI , which is introduced in view of the results of Ref. [8]. The currents in the TF coils are presented further in a form $I_{TFC} \pm \Delta I$ with a plus sign for the inner two coils in each field period and with a minus sign for the outer two coils (ΔI is also expressed in units of the helical winding current).

(iii) f_{VFC} , a multiplying factor for the currents in the VF coils. This factor is connected to an additional vertical magnetic field. It enters linearly into the expression for the magnetic field of the VF coils in a way that for $k_{\varphi}=0.375$ it results in $B_{\perp}/B_0 = 2.5\%$ for $f_{VFC} = 1$, $B_{\perp}/B_0 = 0$ for $f_{VFC} = 1.166$ and $B_{\perp}/B_0 = -2.5\%$ for $f_{VFC} = 1.332$. Here, B_{\perp} is the resulting vertical magnetic field and B_0 is the mean toroidal magnetic field.

Here we focus on results for the studies of the total stored energy for a decreased parameter k_{φ} . Decreasing k_{φ} may reduce the helical ripple, may lead to an improvement of the stored energy in the $1/\nu$ transport regime and a reduction of the magnetic island structure produced by current-feeds and detachable joints of the helical winding.

In Fig. 1 results for $\epsilon_{eff}^{3/2}$ corresponding to $k_{\varphi} \approx 0.31$ for $f_{VFC} = 1$ and 1.166 are presented. The latter value corresponds to a full compensation of the mean vertical magnetic field of the helical winding. Besides, curve 3 shows the results corresponding to $\Delta I \neq 0$ ($f_{VFC} = 1$, $k_{\varphi} \approx 0.31$). For comparison, the results for the standard configuration ($f_{VFC} = 1$, $\Delta I = 0$) are shown.

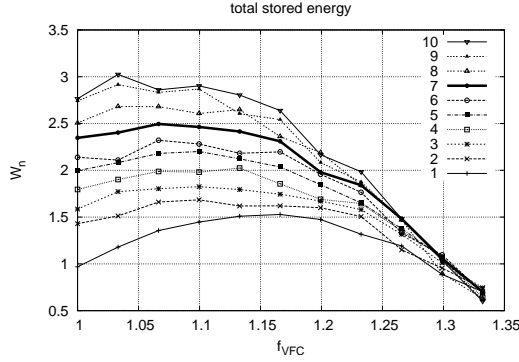


Fig. 2 Re-normalized stored energy (see Eqs. (2) and (3)) for various f_{VFC} (B_{\perp}/B_0) and I_{TFC} (k_{φ}) with taking into account limitations by the chamber; 1: $I_{TFC} = 0.41667$ ($k_{\varphi} = 0.375$); 2: $I_{TFC} = 0.43928$ ($k_{\varphi} = 0.33627$); 3: $I_{TFC} = 0.4619$ ($k_{\varphi} = 0.3512$); 4: $I_{TFC} = 0.4845$ ($k_{\varphi} = 0.3404$); 5: $I_{TFC} = 0.5071$ ($k_{\varphi} = 0.3302$); 6: $I_{TFC} = 0.5298$ ($k_{\varphi} = 0.3206$); 7: $I_{TFC} = 0.55555$ ($k_{\varphi} = 0.3103$); 8: $I_{TFC} = 0.5976$ ($k_{\varphi} = 0.2949$); 9: $I_{TFC} = 0.62024$ ($k_{\varphi} = 0.2873$); 10: $I_{TFC} = 0.6429$ ($k_{\varphi} = 0.28$). (taken from [1])

It can be seen in Fig. 2 that with decreasing k_{φ} the stored energy increases and the maxima in the stored energy correspond to some optimum values of f_{VFC} (B_{\perp}). For $k_{\varphi} \approx 0.31$ (thick line in Fig. 2) it follows that the maximum in the stored energy is approximately $2.5/1.5 \approx 1.65$ times higher than the corresponding maximum for $k_{\varphi} = 0.375$. The results corresponding to $I_{TFC} = 5/9$ ($k_{\varphi} \approx 0.31$) are of special interest because it follows from Ref. [11] that for $k_{\varphi} \approx 0.31$ the magnetic configuration of U-2M is less sensitive to the influence of current-feeds and detachable joints of the helical winding. It has been shown that in this case for the major part of the configuration the rotational transform stays within the range $1/3 < \iota < 1/2$ and big magnetic islands are absent.

The medium size heliac TJ-II ($R = 1.5$ m, $a < 0.2$ m) has four field periods [9] and consists of 32 helically displaced toroidal coils, one central helical coil wrapped around the central circular coil and two vertical field coils. The free parameters for the “common” TJ-II operation are (1) the toroidal coil current, (2) the current for the helical winding, (3) the current for the central circular coil and (4) the current for vertical field coils. For a run of the optimizer these parameters have been varied within the range of $\pm 20\%$ of the corresponding values for the standard configuration, which is within the technical constraints. Within the frame of optimization several configurations with enhanced stored energy compared to the standard configuration could be found. The re-normalized stored energy, defined in Eq. (3) is shown in Fig. 3. It can be seen, that the energy of the best configuration is about 1.45 times as high as the the energy of the standard configuration.

The radial dependency of ϵ_{eff} on the effective radius is presented in Fig. 4. It can be seen that the effective ripple

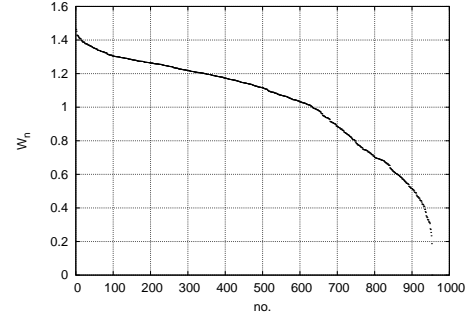


Fig. 3 The re-normalized stored energy (see Eqs. (2) and (3)) for the computed TJ-II configurations (taken from [4]).

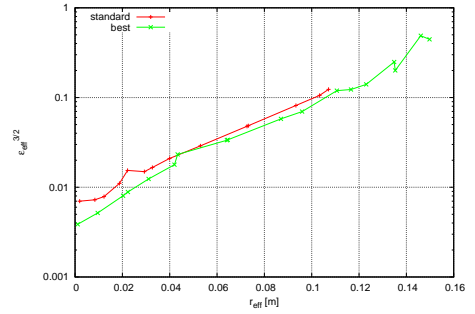


Fig. 4 Effective ripple $\epsilon_{\text{eff}}^{3/2}$ vs. effective radius r_{eff} for TJ-II standard configuration and the best configuration (taken from [4]).

of the best configuration is slightly smaller compared to the standard configuration. Furthermore, the plasma radius of the best configuration ($a \approx 15$ cm) is markedly increased compared to the standard configuration ($a \approx 11$ cm).

The CNT was designed as a simple and compact stellarator with only two pairs of circular, planar coils [10]. These are one pair of interlocking (IL) coils inside the vacuum vessel and another pair of coils, the poloidal field (PF) coils, outside the vacuum vessel. The achieved design goals have been the error field resilience, a large flux surface volume relative to the experimental footprint and that it should be easy to build the experiment. However, minimizing the neoclassical transport was not a design goal. The two free parameters for the optimization are the current of the poloidal field coils (I_{PF}) and the angle between the interlocking coils, called tilt angle. The current for the interlocking coils is fixed at 170 kA which is the design current (see [10]). The two dimensional grid spanned by the PF coil current and the tilt angle has been scanned to get a good knowledge how the re-normalized stored energy W_n depends on the two free parameters. Two different values of the coil separation, which is the vertical distance between the centers of the two IL coils, have been used. One scan was done for the nominal value with 63 cm. The other scan was done for a IL coil separation of 62.6 cm, because for 64 deg tilt angle the edges of the two IL coils would touch each other if they were at the 63 cm coil sep-

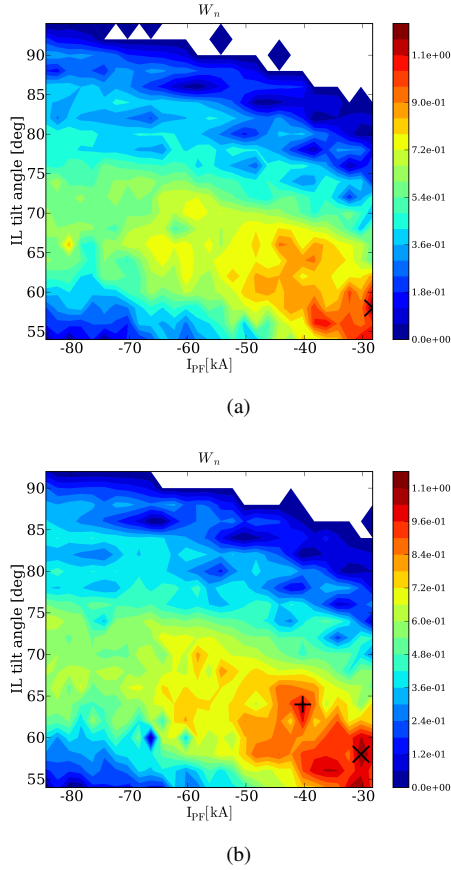


Fig. 5 The re-normalized stored energy for CNT (see Eqs. (2) and (3)) for 63 cm coil separation (a) and 62.6 cm coil separation (b) (taken from [5]). The standard configuration is marked with “+” and the best configuration of each scan is marked with “x”.

eration. The results of these scans are presented in Fig. 5. From these plots can be seen, that W_n is increasing when approaching the area where the PF coil current is -30 kA and the tilt angle is 58 deg. Configurations where the tilt angle is about 90 deg and the PF coil current is in the range of -60 to -30 kA consist mainly of islands and stochastic zones.

The best configuration with a coil separation of 63 cm (referred as “best 630”) exhibits an energy which is enhanced by 17% compared to the standard configuration. The energy of the best configuration with 62.6 cm coil separation (referred as “best 626”) is about 1.1 times the energy of the standard configuration. The standard configuration exhibits the lowest values of ϵ_{eff} of the three considered configurations. The plasma radius for the standard configuration is slightly smaller compared to the plasma radii of the two other configurations. The positive volume effect is stronger than the negative effect of an increased ϵ_{eff} so that the stored energy is higher for the best configurations compared to the stored energy of the standard configuration.

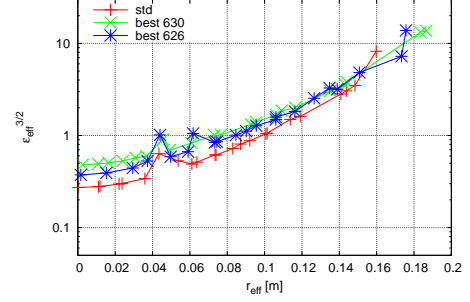


Fig. 6 Effective ripple $\epsilon_{\text{eff}}^{3/2}$ vs. effective radius r_{eff} for the standard configuration and the best configurations for the two considered coil separations (taken from [5]).

4 Conclusion

A scheme for optimizing stellarators in real space with respect to the total stored energy based on neoclassical transport, has been developed and implemented numerically in the code SORSSA. Applying SORSSA to the fusion devices U-2M, TJ-II and CNT, it could be shown that, with a proper choice of the free parameters, configurations with enhanced total stored energy compared to well known standard configurations could be achieved.

- [1] B. Seiwald, V. N. Kalyuzhnyj, S. V. Kasilov, W. Kernbichler, and V. V. Nemov, *Fusion Science and Technology*, 50(3):447–456, 2006.
- [2] G. Grieger, W. Lotz, P. Merkel, J. Nührenberg, et al., *Phys. Fluids B*, 4(7):2081–2091, 1992.
- [3] V. V. Nemov, S. V. Kasilov, W. Kernbichler, and M. F. Heyn, *Phys. Plasmas*, 6(12):4622–4632, 1999.
- [4] B. Seiwald, S. V. Kasilov, W. Kernbichler, V. N. Kalyuzhnyj, V. V. Nemov, V. Tribaldos, and J. A. Jiménez, *J. Comput. Phys.*, 2007. submitted.
- [5] B. Seiwald, V. V. Nemov, T. Sunn Pedersen, and W. Kernbichler, *Plasma Phys. Control. Fusion*, 2007. submitted.
- [6] O. S. Pavlichenko, *Plasma Phys. Control. Fusion*, 35:B223–B230, 1993.
- [7] V. E. Bykov, E. D. Volkov, A. V. Georgievskij, et al., In *Plasma Physics and Controlled Nuclear Fusion Research 1988 (Proc. of 12th Int. Conf., Nice, 1988)*, volume 2, pages 403–410, 1989.
- [8] C. D. Beidler, N. T. Besedin, V. E. Bykov, et al., In *Plasma physics and controlled nuclear fusion research 1990. V. 2. Proceedings of the thirteenth international conference. Vienna (Austria). Washington, D.C., 1 – 6 Oct 1990.*, pages 663 – 675. IAEA, 1991.
- [9] C. Alejaldre, J. J. A. Gozalo, J. Botija Perez, et al., *Fusion Technol.*, 17:131–139, 1990.
- [10] T. Sunn Pedersen, A.H. Boozer, J. P. Kremer, R. G. Lefrancois, W. T. Reiersen, F. Dahlgren, and N. Pomphrey, *Fusion Science and Technology*, 46:200, 2004.
- [11] G. G. Lesnyakov, D. D. Pogozhev, et al., in 23rd EPS Conference on Controlled Fusion and Plasma Physics, 24–28 June 1996, Bogolyubov Institute for Theoretical Physics, Kiev, Ukraine, (European Physical Society, 1996), Vol.20 C, Part II, p.547 (Report b025).